An Optimization-Based Topology Error Detection Method for Power System State Estimation

An Optimization-Based Topology Error Detection Method for Power System State Estimation

Ankur Srivastava[a], Saikat Chakrabarti[b], Joao Soares[c], Sri Niwas Singh[b]

[a]*Division of Electric Power Engineering, Department of Electrical Engineering, Chalmers University of Technology, Gothenburg, 41296, Sweden*
[b]*Department of Electrical Engineering, Indian Institute of Technology, Kanpur, 208016, UP, India*
[c]*GECAD, Polytechnic of Porto, Porto, Portugal*

Abstract

The paper presents an optimization-based method for topology error detection in power systems. The method utilizes the residual analysis in state estimation and minimization of normalized measurement residual, with the application of matrix inverse lemma. The work considers a hybrid measurement configuration, i.e., both SCADA and PMU measurements, for the test systems studied. The proposed method is implemented on the TOMLAB optimization platform under the mixed integer nonlinear programming category. The proposed method has been applied and tested on standard IEEE 14-bus and IEEE 118-bus test systems. The method is designed to be computationally efficient and produces accurate results for single topology error detection. The results from the IEEE 14-bus and IEEE 118-bus test systems have shown that the proposed method produces 100% and 94% accurate results for single topology error detection, respectively. The proposed method performs robustly with the increased measurement uncertainties and inclusion of bad data or gross errors in the measurements. The method has superiority in practical implementation over the meta-heuristics-based optimization methods. The proposed method can be easily implemented and could have potential application in the energy management systems of the power system control center.

Keywords: Network topology, optimization, phasor measurement units, state estimation, topology error detection

1. Introduction

Topology processing is an integral and vital component of power system state estimators (SEs). The topology processing module processes the measurements to determine the physical architecture (interconnection of nodes) of the given network and any electrical island present in the network [1]. Any error in topology may lead to the wrong calculation of the state vector and divergence of the state estimation algorithm [2, 3]. Topology errors may also lead to erroneous results in bad data

identification and wrong database for further analysis of power systems [4]. Topology errors can also cause an economic impact in real-time power markets due to the change in the locational marginal price [5].

Topology error detection methods proposed in the literature can be broadly classified into two general approaches: (l) numerical methods (analytical approaches), and (2) rule-based methods [6]. The majority of the numerical methods depend on conventional SE algorithms. The most commonly used state estimation algorithm is the weighted least squares (WLS) algorithm [1]. The error detection methods used are either pre-processed or post-processed in usual state estimation.

The topology error detection problem was primarily viewed from the perspective of statistical analysis; however, later the problem was also approached with geometric and normalized residuals perspectives. In [7], a method was proposed which improves the SE performance by considering topological errors in the network model used. In [8], a method was developed for the detection of topology errors by using a geometric interpretation of the measurement residuals, and this method was extended further to multiple topology error detection. In [9], the normalized residuals from state estimation results are used to detect topological errors and then a unified model with consideration of these errors is developed.

Further, some researchers also addressed the topology error processing problem with a hybrid approach, including both numerical and rule-based approaches. In [6], to calculate the bus voltage angles, the classification of the measurement data is done by using consistency checks and a network search based on a set of accurate measurements. Thereafter, the measured and calculated data are used for the detection of topology errors. A method is proposed in [10], which estimates the status of the suspected erroneous network elements. The method depends on the results of least absolute value (LAV) SE, which has been proposed as an alternate to WLS SE, for better handling of bad data. Similarly, an algorithm is proposed in [11] for the detection of modest topological errors by using a nonlinear LAV SE with local search algorithms. The normalized Lagrange multipliers are used in [12] for the detection of topology errors. The normalized residual method forms the basis for this method. The method proposed in [13] also uses normalized Lagrange multipliers to identify the topology errors with the consideration of bad data and inaccurate network parameters. In [14], a new state estimation method is proposed based on conventional WLS formulation, which considers the status of circuit breakers as state variables. In [15], a Bayesian-based hypothesis testing procedure is developed and applied to topology error processing via normalized Lagrange multipliers. The research work in [16] has proposed a method based on hypothesis testing for topology error detection. This approach is based on residuals which are obtained by comparing the original measurement with the recovered power flows by solving the network tree. In [17], a method is proposed for topology determination, bad data processing, and state estimation based on a fuzzy clustering [18] and pattern matching technique. A method is proposed for topology processing with PMU measurements in the case

of partially observed networks in [19]. An exhaustive search based topology error detection method for PMUs-only observable system is proposed in [20] along with its validation in a real-time digital simulator. A topology error detection method has been proposed in [21], which uses fully distributed algorithms over convexified problem formulations to achieve scalability and near-global optimal solutions.

The recent approaches show the use of optimization techniques in the detection of topological errors. In [22], an optimization algorithm is used for the strategic placement of phasor measurement units (PMU) and traditional measurements in order to enhance topology error processing capability. A method has been proposed to enhance the accuracy of the network topology optimization in [21]. For the detection of topology errors, heuristic method-based approaches are used. Similarly, the research works in [23] and [24] present particle swarm optimization [25] and binary bat algorithm-based methods for the detection of topological errors. The computational intelligence-based optimization methods have some commonly known challenges such as, i) the difficulty in tuning the optimization parameters, ii) considerably higher number of iterations to converge and give the global optimal solution when the size of the problem increases, and iii) system dependency and different performance under different conditions. Keeping in mind these challenges in the practical implementation of such computational intelligence-based optimization methods, a conventional optimization-based topology error detection method is proposed in this paper. The main contributions of the paper can be summarized as follows:

- Proposing a conventional optimization-based topology error detection method for systems with hybrid measurements, i.e., measurement set consisting of both supervisory control and data acquisition (SCADA) [26] and PMU measurements [27].

- Designing a computationally efficient optimization-based topology error detection method by application of the matrix inverse lemma. The proposed optimization-based topology error detection method is implemented in TOMLAB optimization platform using glcDirect solver.

The rest of the paper is organized as follows. Section 2 describes state estimation-based topology error detection analysis. The problem formulation for topology error detection is explained in Section 3. Section 4 presents the proposed method for topology error detection. Section 5 presents the simulation setup and case studies. Results are discussed in Section 6. Concluding remarks are outlined in Section 7.

2. State Estimation-based Topology Error Detection Analysis

This section reviews the details of topology error detection using SE residuals. Further, the concept and procedure of detection of critical branch and critical pair of branches are discussed. Their pre-calculation helps in reducing the candidates for topological errors in the optimization problem.

2.1. SE Residual Analysis

Linearized measurement equations for WLS SE can be written as [1],

$$\Delta \mathbf{z} = \mathbf{H}\Delta \mathbf{x} + \mathbf{e} \tag{1}$$

where $\Delta \mathbf{z}$ is the active power measurement mismatch vector, $\mathbf{H}$ is the decoupled Jacobian matrix, $\mathbf{e}$ is the noise or measurement error vector, and $\Delta \mathbf{x}$ is the incremental state vector (phase angles).

The estimate, $\Delta \hat{\mathbf{x}}$, of the linearized state vector in WLS SE is given by [1],

$$\Delta \hat{\mathbf{x}} = (\mathbf{H}^T \mathbf{R}^{-1} \mathbf{H})^{-1} (\mathbf{H}^T \mathbf{R}^{-1} \Delta \mathbf{z}) \tag{2}$$

where $\mathbf{R}^{-1}$ is the diagonal weight matrix.

Measurement residual vector, $\mathbf{r}$, can be expressed as [1],

$$\mathbf{r} = \Delta \mathbf{z} - \Delta \hat{\mathbf{z}} = \Delta \mathbf{z} - \mathbf{H}\Delta \hat{\mathbf{x}} \tag{3}$$

Substituting $\Delta \hat{\mathbf{x}}$ from (2) in the above expression, one gets,

$$\mathbf{r} = \Delta \mathbf{z} - \mathbf{H}(\mathbf{H}^T \mathbf{R}^{-1} \mathbf{H})^{-1} (\mathbf{H}^T \mathbf{R}^{-1} \Delta \mathbf{z}) = [\mathbf{I} - \mathbf{K}] \Delta \mathbf{z} \tag{4}$$

where $\mathbf{K} = \mathbf{H}(\mathbf{H}^T \mathbf{R}^{-1} \mathbf{H})^{-1} \mathbf{H}^T \mathbf{R}^{-1}$ is the so-called *hat* matrix and $\mathbf{I}$ is an identity matrix.

The residual vector, $\mathbf{r}$, and the noise vector, $\mathbf{e}$, can be shown to be related as,

$$\mathbf{r} = [\mathbf{I} - \mathbf{K}]\mathbf{e} = \mathbf{W}\mathbf{e} \tag{5}$$

where $\mathbf{W}$ is the residual sensitivity matrix, given by,

$$\mathbf{W} = \mathbf{I} - (\mathbf{H}(\mathbf{H}^T \mathbf{R}^{-1} \mathbf{H})^{-1} \mathbf{H}^T \mathbf{R}^{-1}) \tag{6}$$

Let there be a single bad measurement in the measurement set, viz., the ath one. Let the ath element of the vector, $\mathbf{e}$, be e_a; the remaining elements being zeros. Then the residual vector will be,

$$\mathbf{r} = \mathbf{w}_a e_a \tag{7}$$

where $\mathbf{w}_a$ represents the ath column of the matrix, $\mathbf{W}$.

The above shows that residual vector, $\mathbf{r}$, must be collinear with the column of $\mathbf{W}$, which corresponds to the bad measurement.

The observation on the measurement error can be extended to the topology errors as well [8]. The measurements, $\mathbf{z}$, can be expressed as functions of the states, $\mathbf{x}$, as

$$\mathbf{z} = \mathbf{a}(\mathbf{x}) + \mathbf{e} \tag{8}$$

where $\mathbf{a}(\mathbf{x})$ is the vector of functions relating the measurements to the states.

The branch flow vector, $\mathbf{b}(\mathbf{x})$, can be related to the measurement function, $\mathbf{a}(\mathbf{x})$, as,

$$\mathbf{a}(\mathbf{x}) = \mathbf{M}\mathbf{b}(\mathbf{x}) \tag{9}$$

where $\mathbf{M}$ is the measurement to branch incidence matrix.

In case of a single branch topology error, the change in branch flow vector, $\Delta\mathbf{b}(\mathbf{x})$, will have all elements as zeros except for the one corresponding to the erroneous branch. Let this error be β_j; the erroneous branch being the jth one. Similar to (7), the residual vector, $\mathbf{r}$, can then be expressed as,

$$\mathbf{r} = \beta\mathbf{W}\mathbf{M}\mathbf{l}_j \tag{10}$$

where $\mathbf{l}_j$ is a vector with the jth element as one and the remaining elements as zeros.

A single branch topology error, therefore, results in a residual vector that is collinear with a column of the product, $\mathbf{WM}$. Consequently, a zero column of the matrix product, $\mathbf{WM}$, corresponds to an undetectable topology error in a branch and it is referred to as a critical branch. While collinear columns of the matrix product, $\mathbf{WM}$, correspond to unidentifiable single topology error in branches, and they are referred to as a critical pair of branches.

2.2. Detection of Critical Branch and Critical Pair of Branches

A critical branch is the one, whose removal from the network renders the network unobservable. A critical pair of branches are two branches, after removal of which, the network becomes unobservable. The preceding subsection showed that a single topology error can be detected by finding the column of the matrix product, $\mathbf{WM}$, which is collinear with the residual vector.

The procedure for the detection of critical branch and critical pair of branches is explained in this subsection. Additionally, the expression of matrix, $\mathbf{W}$, as given by (6), involves inverse operation, which requires significant computational effort, especially for large size or practical power systems [8].

Let us consider a fully observable network with a given measurement set. Let n be the number of buses and m be the number of measurements. The size of the Jacobian matrix, $\mathbf{H}$, for a decoupled state estimation will be $m \times (n-1)$.

The procedure for the selection of measurements within a given measurement configuration in a network is explained here. For a given network configuration, usually, the location of measurements is fixed. Therefore, the objective of measurement selection is to select any such (n-1) measurements from a given measurement set, which can make the network fully observable. This statement holds true for a n-bus system and P $-$ δ decoupled state estimation.

The Jacobian matrix, $\mathbf{H}$, is rearranged as shown below [8].

$$\mathbf{H} = \begin{bmatrix} \mathbf{H}_1 \\ \mathbf{H}_2 \end{bmatrix} \tag{11}$$

where $\mathbf{H}_1$ corresponds to such measurements that it is a square matrix and of full rank.

The size of matrix $\mathbf{H}_1$ will be $(n-1) \times (n-1)$, and the size of matrix $\mathbf{H}_2$ will be $(m-n+1) \times (n-1)$. As matrix $\mathbf{H}_1$ is of full rank, the network is fully observable with these (n-1) measurements. Following matrices are now defined [8].

$$\mathbf{F} = \mathbf{H}_2 \mathbf{H}_1^{-1} \tag{12}$$

$$\mathbf{G} = [-\mathbf{F} \quad \mathbf{I}] \tag{13}$$

The step-wise algorithm for the measurement selection for decomposing the measurement Jacobian matrix in the above manner is presented below [1]. The matrices calculation involved in the process is explained in the 7 with the help of a five-bus test system.

1) Form the measurement to bus incidence matrix, $\mathbf{X}_{m1}$, and the gain matrix, $\mathbf{U} = \mathbf{X}_{m1}^T \mathbf{X}_{m1}$
2) Perform the triangular factorization of gain matrix, $\mathbf{U}$, which results in matrices $\mathbf{C}_U$ and $\mathbf{D}_U$
3) Form the matrix, $\mathbf{P}$, using an inverse of matrix, $\mathbf{C}_U$, considering only non-zero rows of matrix, $\mathbf{D}_U$
4) Consider only the boundary injection measurement at buses where originally injection measurements were not present and form a matrix, $\mathbf{X}_{m2}$
5) Form $\mathbf{B} = \mathbf{X}_{m2} \mathbf{P}^T$ and its reduced echelon form, $\mathbf{E}$

As mentioned in the previous subsection, topology error is reflected by the collinearity of the residual vector with the matrix product, $\mathbf{WM}$. In terms of gain matrix, $\mathbf{G}$, the residual sensitivity matrix, $\mathbf{W}$, can be expressed as,

$$\mathbf{W} = \mathbf{R}\mathbf{G}^T (\mathbf{G}\mathbf{R}\mathbf{G}^T)^{-1} \mathbf{G} \tag{14}$$

Since $\mathbf{R}\mathbf{G}^T$ and $(\mathbf{G}\mathbf{R}\mathbf{G}^T)^{-1}$ are full-rank matrices, collinearity among the residual vector and $\mathbf{WM}$ is equivalent to that among the residual vector and the product, $\mathbf{GM}$. The measurement to branch incidence matrix, $\mathbf{M}$, is now decomposed in the same manner, as shown in (11).

$$\mathbf{M} = \begin{bmatrix} \mathbf{M}_1 \\ \mathbf{M}_2 \end{bmatrix} \tag{15}$$

The product, $\mathbf{GM}$, then becomes [8],

$$\mathbf{GM} = \mathbf{M}_2 - \mathbf{F}\mathbf{M}_1 \tag{16}$$

Instead of analyzing the matrix product, **WM**, which is a tedious task, the product, **GM**, is analyzed to identify the topology errors. Once measurement selection is over, matrices $\mathbf{M}_1$ and $\mathbf{M}_2$ can be calculated and thus matrix product, **GM**, can be calculated, according to (16). The algorithm is illustrated here by considering the IEEE 14-bus test system.

The list of measurements is tabulated in Table 1, where measurement types 1 and 2 represent injection and flow measurements, respectively; and type 3 represents PMU measurements. PMU measurements are further transformed into power injection and power flow measurements.

Table 1: Measurement Configuration for IEEE 14-bus Test System

Measurement Serial	**Measurement Type**	**Measurement Location**
1	1	2
2	1	8
3	1	9
4	1	10
5	3	1-2
6	3	1-5
7	2	4-5
8	2	4-7
9	2	6-11
10	2	6-12
11	2	6-13
12	2	9-10
13	2	13-14
14	3	1
15	1	5
16	1	7
17	1	14

For the chosen system and measurement configuration, the matrix, $\mathbf{H}_1$, corresponds to the measurements numbered from 1 to 13. The measurements numbered from 14 to 17 correspond to the matrix, $\mathbf{H}_2$. To determine critical branch and critical pairs of branches, the matrix product, **GM**, is analyzed. Forming $\mathbf{GM}^T$ for the given system configuration,

$$\mathbf{GM}^T = \begin{array}{c} \\ 1 \\ 2 \\ 3 \\ 4 \\ 5 \\ 6 \\ 7 \\ 8 \\ 9 \\ 10 \\ 11 \\ 12 \\ 13 \\ 14 \\ 15 \\ 16 \\ 17 \\ 18 \\ 19 \\ 20 \end{array} \begin{bmatrix} & & & \\ 0 & -1.0000 & 0 & 0 \\ 0 & 0.8950 & -0.1050 & 0 \\ 0 & 0 & 0 & 0 \\ 0 & 0 & 0 & 0 \\ 0 & -1.0000 & 0 & 0 \\ 0 & 0 & 0 & 0 \\ 0 & 1.1050 & 0.1050 & 0 \\ 0 & -0.5525 & 0.4475 & 0 \\ 0 & -0.5525 & -0.5525 & 0 \\ 0 & 1.0000 & 0 & 0 \\ 0 & 1.5525 & 0.5525 & -1.0000 \\ 0 & 0 & 0.0000 & 0.0000 \\ 0 & -0.5525 & -0.5525 & 1.0000 \\ 0 & 0 & 0 & 0 \\ 0 & -0.5525 & 0.4475 & 0 \\ 0 & -1.5525 & -0.5525 & 1.0000 \\ 0 & 0.5525 & 0.5525 & -1.0000 \\ 0 & -1.5525 & -0.5525 & 1.0000 \\ 0 & 0 & 0 & 0 \\ 0 & -0.5525 & -0.5525 & 1.0000 \end{bmatrix}$$

As discussed in Section 3, all zero rows of the matrix product, $\mathbf{GM}^T$, represent critical branches, which are not single-topology error detectable. Hence, for a given measurement configuration, the critical branches are 3, 4, 6, 12, 14, and 19. While the critical pairs of branches are those rows that are linearly dependent among themselves. Here, the critical pair of branches is (8-15).

3. Topology Error Detection Problem Formulation

This section reviews the normalized residuals method which is most commonly used for topology error detection. Single topology errors are the most common type of topology errors that occur in the network. If a branch outage renders the network unobservable, then that particular branch is called a critical branch. For a given measurement configuration, all critical branches can be pre-calculated, as explained in Section 2.2.

The absolute values of the normalized residuals are likely to increase whenever any topology error occurs in the network. Therefore, if the network is simulated with an individual outage of all possible lines, the one which results in minimum normalized residual, shall be the solution for topology error detection. In other words, for correctly assumed topology, the normalized residual will be the minimum [1].

To obtain such a solution, the following formulation of original Jacobian matrix, $\mathbf{H}$, with an individual outage of all possible lines is used [1]:

$$\mathbf{H}_c = \mathbf{H} + \mathbf{H}_e \tag{17}$$

where $\mathbf{H}$ is the original Jacobian matrix, $\mathbf{H}_e$ is the matrix that contains elements reflecting individual line outage, and $\mathbf{H}_c$ is the Jacobian matrix reflecting correct topology.

State estimation equations, given in (2) and (3), are modified for topology error detection problem as:

$$\Delta\hat{\mathbf{x}}_c = (\mathbf{H}_c^T\mathbf{R}^{-1}\mathbf{H}_c)^{-1}(\mathbf{H}_c^T\mathbf{R}^{-1}\Delta\mathbf{z}_c) \tag{18}$$

$$\mathbf{r}_c = \Delta\mathbf{z}_c - \mathbf{H}_c\Delta\hat{\mathbf{x}}_c \tag{19}$$

where $\Delta\mathbf{z}_c$ is the measurement matrix corresponding to the correct topology of the network.

4. Proposed Method

For problem formulation of topology error detection using the conventional optimization based method, suspicious lines are defined as the lines in which there are no flow measurements and are not critical branches as well. The total number of suspicious lines is N_s.

A binary solution vector, $\mathbf{t}$, is used here. The elements of this vector are either zero (implies line is *in*) or one (implies line is *out*). The number of possible solution vectors, $\mathbf{t}$, is equal to the number of suspicious lines present in the network [20].

Now substituting (17) into (18) and (19):

$$\Delta\hat{\mathbf{x}}_c = [(\mathbf{H} + \mathbf{H}_e)^T\mathbf{R}^{-1}(\mathbf{H} + \mathbf{H}_e)]^{-1}[(\mathbf{H} + \mathbf{H}_e)^T\mathbf{R}^{-1}\Delta\mathbf{z}_c] \tag{20}$$

$$\mathbf{r}_c = \Delta\mathbf{z}_c - [(\mathbf{H} + \mathbf{H}_e)\Delta\hat{\mathbf{x}}_c] \tag{21}$$

In (20) and (21), matrix $\mathbf{H}_e$ is the only variable; other matrices are fixed. If $\mathbf{H_e}$ can be expressed as a direct function of solution vector $\mathbf{t}$, then $\mathbf{r}_c$ also becomes a function of solution vector $\mathbf{t}$. This can be formulated as:

$$\mathbf{H}_e = \mathbf{STY} \tag{22}$$

where $\mathbf{S}$ is a constant incidence matrix relating measurements and suspicious lines; $\mathbf{Y}$ is a constant admittance matrix relating suspicious lines with bus locations, and $\mathbf{T}$ is the diagonal matrix formed by the elements of the solution vector $\mathbf{t}$. For illustration, let us formulate matrices $\mathbf{Y}$ and $\mathbf{S}$ for a test system described in Figure 1.

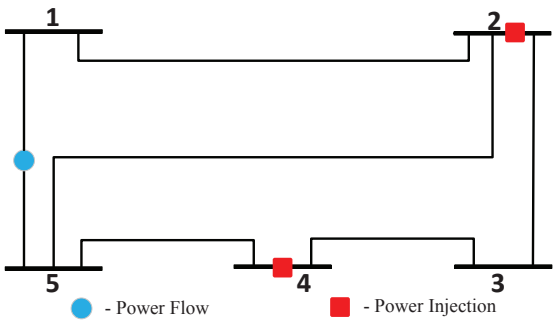

Figure 1: Line diagram of a 5-bus system with measurement set.

1. Formation of matrix, $\mathbf{S}$: The size of matrix $\mathbf{S}$ will be $m \times N_s$, where m is the number of measurements and N_s is the number of suspicious lines. The entries s in each row of matrix $\mathbf{S}$ will be done as:

$$s = \begin{cases} +1, \text{ if the injection is at sending end of the line} \\ -1, \text{ if the injection is at receiving end of the line} \\ 0, \text{ otherwise} \end{cases}$$

$$\mathbf{S} = \begin{array}{c} \\ inj(2) \\ inj(4) \\ flow(1-5) \end{array} \begin{array}{c} \begin{array}{ccccc} N_{s1} & N_{s2} & N_{s3} & N_{s4} & N_{s5} \end{array} \\ \begin{bmatrix} -1 & 1 & 1 & 0 & 0 \\ 0 & 0 & 0 & -1 & 1 \\ 0 & 0 & 0 & 0 & 0 \end{bmatrix} \end{array}$$

2. Formation of matrix, $\mathbf{Y}$: The size of matrix $\mathbf{Y}$ will be $N_s \times n$, where n is the number of buses and N_s is the number of suspicious lines. The entries y in each row of the matrix $\mathbf{Y}$ will be done as:

$$y = \begin{cases} +\mathrm{y}_q, \text{if the bus is sending end of the line} \\ -\mathrm{y}_q, \text{if the bus is receiving end of the line} \\ 0, \text{otherwise} \end{cases}$$

$$\mathbf{Y} = \begin{array}{c} \\ N_{s1}(1-2) \\ N_{s2}(2-3) \\ N_{s3}(2-5) \\ N_{s4}(3-4) \\ N_{s5}(4-5) \end{array} \begin{array}{c} \begin{array}{ccccc} 1 & 2 & 3 & 4 & 5 \end{array} \\ \begin{bmatrix} \mathrm{y}_1 & -\mathrm{y}_1 & 0 & 0 & 0 \\ 0 & \mathrm{y}_3 & -\mathrm{y}_3 & 0 & 0 \\ 0 & \mathrm{y}_4 & 0 & 0 & -\mathrm{y}_4 \\ 0 & 0 & \mathrm{y}_5 & -\mathrm{y}_5 & 0 \\ 0 & 0 & 0 & \mathrm{y}_6 & -\mathrm{y}_6 \end{bmatrix} \end{array}$$

where y_q is the admittance of the considered suspicious line.

Therefore, the objective function along with the constraints can be expressed as:

$$\min \ (\mathbf{r}_c^T \mathbf{r}_c)^{1/2} \tag{23}$$

$$\mathbf{r}_c = \Delta \mathbf{z}_c - \mathbf{H}_c(\mathbf{H}_c^T \mathbf{R}^{-1} \mathbf{H}_c)^{-1}(\mathbf{H}_c^T \mathbf{R}^{-1} \Delta \mathbf{z}_c) \tag{24}$$

Subjected to constraints:

$$\sum_{q=1}^{N_s} \mathbf{t}(q) = 1 \tag{25}$$

where, $\mathbf{t}(q)$ is the qth element of the solution vector, $\mathbf{t}$. The solution vector, $\mathbf{t}$, which gives the minimum value of r will be the desired solution for topology error detection.

In (24), the inverse of the matrix $(\mathbf{H}_c^T \mathbf{R}^{-1} \mathbf{H}_c)$ is required, to find the fresh estimate of state variables and substitute it for evaluation of measurement residuals. The size of the matrix $(\mathbf{H}_c^T \mathbf{R}^{-1} \mathbf{H}_c)$ is $n \times n$, where n is the number of buses. For an nth order matrix, inverse calculations requires n^3 operations. For higher-order systems, where the number of buses is large, it require significant computational effort and involves large truncation errors. Thus, it turns out to be very costly for all mathematical applications and direct inversion of such a huge matrix is avoided. Under certain measurement configurations, the direct matrix inversion method may sometimes fail to give correct results for topological error detection problem, especially when the matrix $(\mathbf{H}_c^T \mathbf{R}^{-1} \mathbf{H}_c)$ tends to become singular.

A matrix inverse lemma-based approach is proposed to avoid matrix inversion calculations. The commonly used form of matrix inverse lemma technique is given as [28]:

$$(\mathbf{A} - \mathbf{B}\mathbf{D}^{-1}\mathbf{C})^{-1} = \mathbf{A}^{-1} + \mathbf{A}^{-1}\mathbf{B}(\mathbf{D} - \mathbf{C}\mathbf{A}^{-1}\mathbf{B})^{-1}\mathbf{C}\mathbf{A}^{-1} \tag{26}$$

Let us substitute (17) into the matrix $(\mathbf{H}_c^T \mathbf{R}^{-1} \mathbf{H}_c)$, and expand:

$$\mathbf{H}_c^T \mathbf{R}^{-1} \mathbf{H}_c = \mathbf{H}^T \mathbf{R}^{-1} \mathbf{H} + \mathbf{H}_e^T \mathbf{R}^{-1} \mathbf{H}_e + \mathbf{H}_e^T \mathbf{R}^{-1} \mathbf{H} + \mathbf{H}^T \mathbf{R}^{-1} \mathbf{H}_e \tag{27}$$

The following notations are used to illustrate the matrix computation process:

$$\mathbf{H}^T \mathbf{R}^{-1} \mathbf{H} + \mathbf{H}_e^T \mathbf{R} \mathbf{H}_e = \mathbf{A}_1 \tag{28}$$

$$\mathbf{H}^T \mathbf{R}^{-1} \mathbf{H} + \mathbf{H}_e^T \mathbf{R}^{-1} \mathbf{H}_e + \mathbf{H}_e^T \mathbf{R}^{-1} \mathbf{H} = \mathbf{A}_1 + \mathbf{H}_e^T \mathbf{R}^{-1} \mathbf{H} = \mathbf{A}_2 \tag{29}$$

$$\mathbf{H}^T \mathbf{R}^{-1} \mathbf{H} + \mathbf{H}_e^T \mathbf{R}^{-1} \mathbf{H}_e + \mathbf{H}_e^T \mathbf{R}^{-1} \mathbf{H} + \mathbf{H}^T \mathbf{R}^{-1} \mathbf{H}_e = \mathbf{A}_2 + \mathbf{H}^T \mathbf{R}^{-1} \mathbf{H}_e = \mathbf{A}_3 \tag{30}$$

Here, in this problem, matrix $\mathbf{H}_e$ is a highly sparse matrix in which only a few elements change from the base case matrix. In (26), to obtain the inverse of a matrix $(\mathbf{A} - \mathbf{B}\mathbf{D}^{-1}\mathbf{C})$, it further requires the inversion of matrix $\mathbf{A}$ and matrix $(\mathbf{D} - \mathbf{C}\mathbf{A}^{-1}\mathbf{B})$.

In the topology error detection problem of (27), matrix $\mathbf{A}$ is equivalent to $\mathbf{H}^T \mathbf{R}^{-1} \mathbf{H}$, which is a known matrix and whose inverse can be pre-calculated and can be used further. Also, the size of the matrix $(\mathbf{D} - \mathbf{C}\mathbf{A}^{-1}\mathbf{B})$ will be the same as that of matrix $\mathbf{D}$. If matrix $\mathbf{D}$ can be expressed as a scalar quantity (with corresponding values of matrix $\mathbf{B}$ and $\mathbf{C}$), then the term $(\mathbf{D} - \mathbf{C}\mathbf{A}^{-1}\mathbf{B})$ will also become a scalar quantity. This detailed problem formulation is presented as follows:

Inversion of $\mathbf{A}_1$ in (28) can be broken in the standard form of inverse lemma technique (26), as follows:

$$\mathrm{A} = \mathbf{H}^T\mathbf{R}^{-1}\mathbf{H},\ \mathrm{B}_1 = \mathbf{H_e}^T,\ \mathrm{D}_1 = \mathbf{R},\ \mathrm{C}_1 = \mathbf{H_e}$$

Further, B_1 and C_1 can be expressed in terms of solution vector, $\mathbf{t}$, as:

$$\mathrm{B}_1 = \mathbf{NQt}^T,\ \mathrm{C}_1 = \mathbf{tQ}^T\mathbf{N}^T$$

Thus,

$$\begin{aligned}\mathbf{A}_1^{-1} &= (\mathbf{A} - \mathbf{B}_1\mathbf{D}_1^{-1}\mathbf{C}_1)^{-1} \\ &= \mathbf{A}^{-1} + \mathbf{A}^{-1}\mathbf{B}_1(\mathbf{D}_1 - \mathbf{C}_1\mathbf{A}^{-1}\mathbf{B}_1)^{-1}\mathbf{C}_1\mathbf{A}^{-1}\end{aligned}$$

Inversion of $\mathbf{A}_2$ in (29) can be broken in the standard form of inverse lemma technique (26), as follows:

$$\mathrm{A}_1 = \mathbf{H}^T\mathbf{R}^{-1}\mathbf{H} + \mathbf{H}_e^T\mathbf{R}^{-1}\mathbf{H}_e,\ \mathrm{B}_2 = \mathbf{H_e}^T,\ \mathrm{D}_2 = \mathbf{R},\ \mathrm{C}_2 = \mathbf{H}$$

Further, B_2 and C_2 can be expressed in terms of solution vector, $\mathbf{t}$, as:

$$\mathrm{B}_2 = \mathbf{NQt}^T,\ \mathrm{C}_2 = \mathbf{tJH}$$

Thus,

$$\begin{aligned}\mathbf{A}_2^{-1} &= (\mathbf{A}_1 - \mathbf{B}_2\mathbf{D}_2^{-1}\mathbf{C}_2)^{-1} \\ &= \mathbf{A}_1^{-1} + \mathbf{A}_1^{-1}\mathbf{B}(\mathbf{D}_2 - \mathbf{C}_2\mathbf{A}_1^{-1}\mathbf{B}_2)^{-1}\mathbf{C}_2\mathbf{A}_1^{-1}\end{aligned}$$

Inversion of $\mathbf{A}_3$ in (30) can be broken in the standard form of inverse lemma technique (26), as follows:

$$\mathrm{A}_2 = \mathbf{H}^T\mathbf{R}^{-1}\mathbf{H} + \mathbf{H}_e^T\mathbf{R}^{-1}\mathbf{H}_e + \mathbf{H}_e^T\mathbf{R}^{-1}\mathbf{H},\ \mathrm{B}_3 = \mathbf{H}^T,\ \mathrm{D}_3 = \mathbf{R},\ \mathrm{C}_3 = \mathbf{H_e}$$

Further, B_3 and C_3 can be expressed in terms of solution vector, $\mathbf{t}$, as:

$$\mathrm{B}_3 = \mathbf{H}^T\mathbf{J}^T\mathbf{t}^T,\ \mathrm{C}_3 = \mathbf{tQ}^T\mathbf{N}^T$$

Thus,

$$\begin{aligned}\mathbf{A}_3^{-1} &= (\mathbf{A}_2 - \mathbf{B}_3\mathbf{D}_3^{-1}\mathbf{C}_3)^{-1} \\ &= \mathbf{A}_2^{-1} + \mathbf{A}_2^{-1}\mathbf{B}_3(\mathbf{D}_3 - \mathbf{C}_3\mathbf{A}_2^{-1}\mathbf{B}_3)^{-1}\mathbf{C}_3\mathbf{A}_2^{-1}\end{aligned}$$

where $\mathbf{N}$ is a constant admittance matrix of size $n \times n_{line}$, which relates line admittances with bus locations; $\mathbf{Q}$ is a constant incidence matrix of size $n_{line} \times N_s$, which relates all the lines with suspicious lines; $\mathbf{J}$ is also a constant incidence matrix of size $N_s \times m$, which relates measurements with suspicious lines and $\mathbf{H}$ is the original Jacobian matrix. Here, n is the number of buses, n_{line} is the total number of lines, N_s is the number of suspicious lines, and m is the number of measurements.

$\mathbf{D}_1$, $\mathbf{D}_2$, and $\mathbf{D}_3$ are scalar quantities that represent the weights assigned to measurements in state estimation. Here, matrices $(\mathbf{D}_1 - \mathbf{C}_1\mathbf{A}^{-1}\mathbf{B}_1)$, $(\mathbf{D}_2 - \mathbf{C}_2\mathbf{A}_1^{-1}\mathbf{B}_2)$, and $(\mathbf{D}_3 - \mathbf{C}_3\mathbf{A}_2^{-1}\mathbf{B}_3)$ are scalar quantities. The matrix $\mathbf{A}_3^{-1}$ corresponds to the desired inverse of the matrix $(\mathbf{H}_c^T\mathbf{R}^{-1}\mathbf{H}_c)$.

5. Simulation Setup and Case Studies

This section presents the simulation setup which includes the optimization and solver setup and case studies for the IEEE 14-bus and IEEE 118-bus test systems [29], to evaluate the performance of the proposed method.

5.1. Optimization and Solver Setup

The objective function of the optimization problem is to minimize the function r and finding the solution vector, $\mathbf{t}$, corresponding to this minimum value of r. The size of the solution vector, $\mathbf{t}$, varies with the size of the test system. For a given measurement configuration, the suspicious lines constitute the possibilities of solution vector, $\mathbf{t}$. The proposed method is implemented in a computer with configuration as Intel(R) Xeon(R) CPU E5-1650@3.20 GHz and 10.0 GB RAM. The implementation is done using MATLAB(R) R2014a and TOMLAB 8.1 toolbox [30]. The optimization model is developed and formulated using the optimization toolbox TOMLAB that offers various optimization categories and solvers. The optimization problem in the proposed method is solved under the mixed integer nonlinear programming (MINLP) category. The glcDirect solver along with its default options is employed in this work. This solver is a modified version of the algorithm DIRECT implemented in [31] for solving a constrained mixed integer global optimization. The original DIRECT algorithm is modified and expanded by TOMLAB for the handling of the nonlinear/linear equalities along with the linear inequalities.

5.2. Case Studies

The proposed method is applied on IEEE 14-bus and IEEE 118-bus test systems [29] whose details along with the measurement configuration are presented as follows:

5.2.1. IEEE 14-bus test system

The measurement details and locations are tabulated in Table 2. While the critical branches and critical pairs of branches are presented in Table 3. For the considered measurement configuration, there are nine flow measurements and six critical branches, with one common line, so there are six suspicious lines.

Table 2: Location of Different Measurements for IEEE 14-bus Test System

Location of injection measurements (SCADA)	**Location of flow measurements (SCADA)**	**Location of PMU measurements**
2, 5, 7, 8, 9, 10, 14	4-5, 4-7, 6-11, 6-12, 6-13, 9-10, 13-14	1 (**Injection**-1, **Flow**- 1-2, 1-5)

Table 3: Critical Lines and Critical Pairs of Lines for IEEE 14-bus Test System

Critical Lines	**Critical Pairs of Lines**
2-3, 2-4, 3-4, 6-12, 7-8, 12-13	(4-7, 7-9)

5.2.2. IEEE 118-bus test system

The measurement details and locations for this test system are tabulated in Table 4. While the critical branches and critical pair of branches are presented in Table 5. For the considered measurement configuration in IEEE 118-bus system [29], there are fifty suspicious lines.

Table 4: Location of Different Measurements for IEEE 118-bus Test System

Location of injection measurements (SCADA)	**Location of flow measurements (SCADA)**	**Location of PMU measurements**
1, 2, 4, 6, 8, 12, 13, 15, 17, 19, 20, 22, 23, 25, 27, 28, 31, 32, 34, 36, 37, 38, 41, 42, 45, 48, 49, 55, 61, 63, 68, 71, 73, 77, 78, 85, 89, 92, 94, 100, 103, 105, 108, 110, 115, 116, 118	1-3, 3-12, 4-5, 5-11, 6-7, 7-12, 8-9, 8-30, 11-12, 12-14, 12-16, 13-15, 15-17, 15-19, 15-33, 16-17, 17-113, 19-20, 22-23, 23-25, 24-70, 24-72, 25-26, 26-30, 27-32, 28-29, 29-31, 32-113, 32-114, 33-37, 34-37, 34-43, 35-36, 35-37, 37-39, 38-65, 39-40, 40-42, 41-42, 43-44, 45-49, 46-48, 47-49, 47-69, 49-54, 49-69, 52-53, 53-54, 54-55, 54-56, 55-56, 56-57, 50-57, 54-59, 60-61, 60-62, 61-62, 61-64, 62-67, 64-65, 65-68, 66-67, 68-81, 69-70, 70-75, 71-72, 74-75, 75-77, 76-118, 76-77, 83-85, 84-85, 85-89, 89-90, 91-92, 92-94, 93-94, 94-95, 94-100, 95-96, 99-100, 100-101, 100-106, 101-102, 103-105, 104-105, 105-106, 106-107, 108-109, 109-110, 114-115	10, 58, 80, 82, 87, 98, 112 (**Injection-**10, 58, 80, 82, 87, 98, 112 **Flow-**9-10, 56-58, 51-58, 77-80, 77-82, 79-80, 80-81, 80-96, 80-97, 80-98, 80-99, 82-83, 82-96, 86-87, 98-100, 110-112)

Table 5: Critical Lines and Critical Pairs of Lines for IEEE 118-bus Test System

Critical Lines	**Critical Pairs of Lines**
3-5, 8-9, 9-10, 12-14, 12-117, 14-15, 46-47, 51-52, 52-53, 53-54, 56-59, 59-60, 59-63, 62-66, 63-64, 65-66, 68-116, 69-75, 70-74, 71-73, 74-75, 80-97, 83-84, 84-85, 85-86, 85-88, 86-87, 88-89, 89-90, 90-91, 91-92, 96-97, 110-111, 110-112	(1-2, 2-12) (1-3, 3-12) (4-5, 4-11) (11-13, 13-15) (12-16, 16-17) (15-33, 33-37) (25-26, 26-30) (32-113, 17-113) (37-39, 39-40) (40-41, 41-42) (54-55, 55-59) (68-81, 80-81) (80-98, 98-100) (94-95, 95-96) (100-103, 104-105) (105-107, 106-107)

5.3. Consideration of Measurement Uncertainties

The measurement meters are installed in the field and the measurements are received through communication channels, which leads to unwanted phenomena such as the addition of noise, data packet loss, etc., making the measurements contaminated. To incorporate the noise, uncertainties are added to the measurements without the loss of generality. It is simulated by adding uncertainties based on the Gaussian distribution associated with the type of measurements. Further, the added Gaussian noise has zero mean and the maximum measurement uncertainties associated with the different type of measurements are shown in Table 6 [32]. To analyze the impact of measurement uncertainties on the accuracy of the proposed method, additional case studies with increased measurement uncertainties are performed. The maximum measurement uncertainties associated with different measurement types for the additional case studies are presented in Table 7.

Table 6: Standard Maximum Measurement Uncertainties Associated with Different Measurement Types

Measurement Type	**SCADA Measurements**		**PMU Measurements**	
	Power Injection	Power Flow	Voltage	Current
Maximum Uncertainty	3%	3%	0.02%	0.03%

Table 7: Maximum Measurement Uncertainties Associated with Different Measurement Types for Additional Case Studies

Sl. No.	**Measurement Uncertainty**			
	SCADA Measurements		**PMU Measurements**	
	Power Injection	Power Flow	Voltage	Current
Case Study 1	4%	4%	0.03%	0.04%
Case Study 2	5%	5%	0.04%	0.05%

6. Results and Discussion

This section presents the results obtained through the application of the proposed method for topology error detection in IEEE 14-bus and IEEE 118-bus test systems. The software-based TOMLAB optimization platform is employed in the proposed method to solve the topology error detection problem.

6.1. Accuracy of the Proposed Method

This subsection presents the accuracy of the proposed method under different case studies such as standard measurement uncertainties, increased measurement uncertainties, and, inclusion of bad data.

6.1.1. With Standard Measurement Uncertainties

The results for all possible cases of topology error detection with IEEE 14-bus and IEEE 118-bus test systems for a given measurement configuration are presented in Table 8. While the percentage accuracy obtained using the proposed method (in case of the single topology error detection) for IEEE 14-bus and IEEE 118-bus test systems is presented in Figure 2.

Table 8: Results of Topology Error Detection with the Proposed Method for IEEE 14-bus and IEEE 118-bus Test Systems

Methods	IEEE 14-bus	IEEE 118-bus
Possible cases	6	50
Number of cases with correct detection	6	47

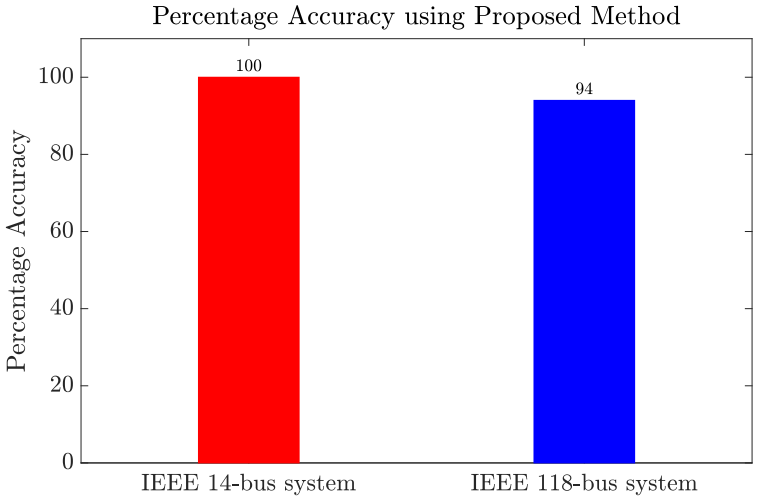

Figure 2: Percentage accuracy for topology error detection using the proposed method with IEEE 14-bus and IEEE 118-bus test systems.

It can be seen from Figure 2 that the proposed matrix inverse lemma-based conventional optimization method produces 100% and 94% correct results for single topology error detection with IEEE 14-bus and IEEE 118-bus test systems, respectively. The reason behind such high accuracy is the capability of the proposed method to handle large inverse operations. The impact of large inverse operations on the accuracy will be less significant in the case of small test systems. But as the size of the system increases, the direct inversion process becomes more tedious and produces high truncation errors which could lead to wrong results. As presented in Figure 2, the proposed method performs well with both IEEE 14-bus and IEEE 118-bus test systems and thus its performance remains largely independent of the size of the test system. The proposed method shall give similar percentage accuracy with the increase in the size of the network.

6.1.2. With Increased Measurement Uncertainties

Measurement uncertainties may have an impact on the accuracy of the proposed topology error detection method. In order to test the performance of the proposed method under such conditions, case studies are performed with different maximum measurement uncertainties as presented in Table 7. The results obtained with both case studies have shown the same percentage accuracy as in the previous subsection. The proposed method in these case studies have produced 100% and 94% correct results for single topology error detection with IEEE 14-bus and IEEE 118-bus test systems, respectively. The results of these case studies confirm the robustness of the proposed topology error detection method in case of increased measurement uncertainties or higher measurement noise.

6.1.3. With Inclusion of Bad Data or Gross Errors

The proposed method is tested with the inclusion of bad data or gross errors in the measurement set. This effect is simulated by randomly selecting and contaminating 2 and 18 number of measurements in IEEE 14-bus and IEEE 118-bus test systems, respectively. After measurement selection, uncertainties in the range of $10 - 20\%$ are added randomly to these measurements [33]. All possible cases of topology error detection with IEEE 14-bus and IEEE 118-bus test systems are simulated with the inclusion of bad data. There is no substantial impact of bad data or gross errors on the accuracy of the proposed method and the same percentage accuracy level is achieved in both IEEE 14-bus and IEEE 118-bus test systems.

6.2. Execution Time of the Proposed Method

The average TOMLAB execution time for the IEEE 14-bus and IEEE 118-bus test systems are presented in Table 9. The execution time is further classified under three categories as symbolic processing, elapsed, and CPU time.

1. *Symbolic processing time* refers to the initial setup of the problem formulation.

2. *Elapsed time* refers to the effective time spent by the solver to converge and reach the best found solution.

3. *CPU time* refers to the total time spent by each processor thread (parallel processing).

The CPU time is in principle higher than the elapsed time since it accounts for the aggregated sum of the time spent by each thread that processes the parts of the glcDirect solver.

It can be seen from Table 9 that the symbolic processing time are similar in case of IEEE 14-bus and IEEE 118-bus test systems. It also shows that the symbolic processing time has a minor impact in the overall computation time. Further, the average elapsed time and CPU time increases with the size of the test system which is expected due to processing of larger matrices and more possibilities for the candidates. However, the average elapsed time comes out as 0.1368 seconds and the average CPU time comes as 0.8512 seconds which is within the acceptable range.

Table 9: Average Execution Time with the Proposed Method for IEEE 14-bus and IEEE 118-bus Test Systems (in Seconds)

Category	**IEEE 14-bus**	**IEEE 118-bus**
Symbolic Processing Time	0.0848	0.0950
Elapsed Time	0.0190	0.1368
CPU Time	0.0219	0.8512

7. Conclusion

A methodology for topology error detection for power systems is proposed in this paper. The method is based on residual analysis in state estimation and minimization of normal residual. The proposed method utilizes the matrix inverse lemma method and a conventional optimization method. The conventional optimization formulation is implemented on the TOMLAB optimization platform under the mixed integer nonlinear programming category. The proposed method is applied to standard IEEE 14-bus and IEEE 118-bus test systems. The method performed adequately and produced results with high percentage accuracy for topology error detection in case of both test systems. The proposed method also performed robustly with the increased measurement uncertainties and inclusion of bad data or gross errors in the measurement set. The method is designed to perform in a computationally efficient manner and thus it has potential application in power system monitoring and control. The results of topology error detection have a direct impact on the output of state estimation, which in turn is very important for system security and reliability.

The extension of the method to detect multiple topology errors under various other measurement configurations is planned for future studies.

Acknowledgement

This work was supported by the Department of Science and Technology, India, and Central Power Research Institute, India under project no. DST/EE/2014250 and CPRI/EE/2014091, respectively.

References

[1] A. Abur, A. G. Exposito, Power system state estimation: theory and implementation, CRC press, 2004.

[2] W.-H. Liu, S.-L. Lim, Parameter error identification and estimation in power system state estimation, IEEE Transactions on Power Systems 10 (1) (1995) 200–209.

[3] M. Irving, Robust algorithm for generalized state estimation, IEEE Transactions on Power Systems 24 (4) (2009) 1886–1887.

[4] N. Singh, H. Glavitsch, Detection and identification of topological errors in online power system analysis, IEEE Transactions on Power Systems 6 (1) (1991) 324–331.

[5] D.-H. Choi, L. Xie, Impact of power system network topology errors on real-time locational marginal price, Journal of Modern Power Systems and Clean Energy 5 (5) (2017) 797–809.

[6] C. Lu, J. Teng, B. Chang, Power system network topology error detection, IEE Proceedings-Generation, Transmission and Distribution 141 (6) (1994) 623–629.

[7] R. Lugtu, D. Hackett, K. Liu, D. Might, Power system state estimation: Detection of topological errors, IEEE Transactions on Power Apparatus and Systems (6) (1980) 2406–2412.

[8] K. Clements, P. Davis, Detection and identification of topology errors in electric power systems, IEEE Transactions on Power Systems 3 (4) (1988) 1748–1753.

[9] F. F. Wu, W.-H. Liu, Detection of topology errors by state estimation, IEEE Transactions on Power Systems 4 (1) (1989) 176–183.

[10] H. Singh, F. L. Alvarado, Network topology determination using least absolute value state estimation, IEEE Transactions on Power Systems 10 (3) (1995) 1159–1165.

[11] S. W. Park, R. Mohammadi-Ghazi, J. Lavaei, Topology error detection and robust state estimation using nonlinear least absolute value, in: Proc. IEEE American Control Conference (ACC), 2019, pp. 5505–5512.

[12] K. A. Clements, A. S. Costa, Topology error identification using normalized lagrange multipliers, IEEE Transactions on Power Systems 13 (2) (1998) 347–353.

[13] M. Kabiri, N. Amjady, Improving topology error identification through considering parameter and measurement errors, International Journal of Electrical Power & Energy Systems 97 (2018) 309–318.

[14] G. N. Korres, P. J. Katsikas, Identification of circuit breaker statuses in WLS state estimator, IEEE Transactions on Power Systems 17 (3) (2002) 818–825.

[15] E. M. Lourenco, A. S. Costa, K. A. Clements, Bayesian-based hypothesis testing for topology error identification in generalized state estimation, IEEE Transactions on Power Systems 19 (2) (2004) 1206–1215.

[16] W. B. Wu, M. X. Cheng, B. Gou, A hypothesis testing approach for topology error detection in power grids, IEEE Internet of Things Journal 3 (6) (2016) 979–985.

[17] D. Singh, J. Pandey, D. Chauhan, Topology identification, bad data processing, and state estimation using fuzzy pattern matching, IEEE Transactions on Power Systems 20 (3) (2005) 1570–1579.

[18] D. E. Gustafson, W. C. Kessel, Fuzzy clustering with a fuzzy covariance matrix, in: Proc. IEEE conference on decision and control including the 17th symposium on adaptive processes, 1979, pp. 761–766.

[19] E. Mohamed, W. Elballa, A. Karrar, G. Kobet, A. Eltom, Fast line outage detection using PMU measurements in partially observed networks, in: Proc. IEEE Power & Energy Society General Meeting (PESGM), 2018, pp. 1–5.

[20] A. Srivastava, A. Dubey, S. Chakrabarti, An exhaustive search based topology error detection method and its validation in real time digital simulator, in: Proc. IEEE Region 10 Conference (TENCON), Nov. 2017, pp. 534–539.

[21] Y. Weng, M. D. Ilić, Q. Li, R. Negi, Distributed algorithms for convexified bad data and topology error detection and identification problems, International Journal of Electrical Power & Energy Systems 83 (2016) 241–250.

[22] J. Chen, A. Abur, Enhanced topology error processing via optimal measurement design, IEEE Transactions on Power Systems 23 (3) (2008) 845–852.

[23] N. K. Sharma, S. Chakrabarti, An optimization based method for topology error detection for state estimation, in: Proc. IEEE Innovative Smart Grid Technologies Asia (ISGT ASIA), Nov. 2015, pp. 1–6.

[24] A. A. Hossam-Eldin, E. N. Abdallah, A. H. Kassem, K. H. Youssef, Relevant subnetwork identification for topology error detection in power systems, in: Proc. 2018 IEEE International Conference on Environment and Electrical Engineering and 2018 IEEE Industrial and Commercial Power Systems Europe (EEEIC/I&CPS Europe), 2018, pp. 1–6.

[25] J. Kennedy, R. Eberhart, Particle swarm optimization, in: Proc. IEEE ICNN'95-international conference on neural networks, Vol. 4, 1995, pp. 1942–1948.

[26] S. A. Boyer, SCADA: supervisory control and data acquisition, International Society of Automation, 2009.

[27] A. G. Phadke, J. S. Thorp, Synchronized phasor measurements and their applications, Vol. 1, Springer, 2008.

[28] D. J. Tylavsky, G. R. Sohie, Generalization of the matrix inversion lemma, Proceedings of the IEEE 74 (7) (1986) 1050–1052.

[29] R. Christie, Power system test archive, University of Washington (1999).

[30] TOMLAB Optimization AB, Västerås, Sweden [Online]. Available: https://www.tomopt.com/ (2006).

[31] D. R. Jones, Encyclopedia of optimization, Kluwer Academic Publishers (2001).

[32] S. Chakrabarti, E. Kyriakides, G. Valverde, V. Terzija, State estimation including synchronized measurements, in: Proc. IEEE Bucharest PowerTech, June 2009, pp. 1–5.

[33] J. Chen, A. Abur, Placement of PMUs to enable bad data detection in state estimation, IEEE Transactions on Power Systems 21 (4) (2006) 1608–1615.

Appendix A. Measurement Placement Example

Here the problem of measurement placement as presented in Section 2.2 is illustrated with a test case.

Consider an example of a five-bus system. A single line diagram for a test system with five bus and six lines along with two power injection and one power flow measurement is shown in Figure 1.

The various matrices for measurement selection algorithm in the case of this test system are as follows:

$$\mathbf{X}_{m1} = \begin{bmatrix} -1 & 3 & -1 & 0 & -1 \\ 1 & 0 & 0 & 0 & -1 \\ 0 & 0 & -1 & 2 & -1 \end{bmatrix}, \mathbf{U} = \begin{bmatrix} 2 & -3 & 1 & 0 & 0 \\ -3 & 9 & -3 & 0 & -3 \\ 1 & -3 & 2 & -2 & 2 \\ 0 & 0 & -2 & 4 & -2 \\ 0 & -3 & 2 & -2 & 3 \end{bmatrix}$$

$$\mathbf{C} = \begin{bmatrix} 1 & & & & \\ -1.5 & 1 & & & \\ 0.5 & -0.33 & 1 & & \\ 0 & 0 & -2 & 1 & \\ 0 & -0.67 & 1 & 0 & 1 \end{bmatrix}, \mathbf{D} = \begin{bmatrix} 2 & & & & \\ & 4.5 & & & \\ & & 1 & & \\ & & & 0 & \\ & & & & 0 \end{bmatrix}, \mathbf{P} = \begin{bmatrix} 0 & 0.67 & 2 & 1 & 0 \\ 1 & 0.33 & -1 & 0 & 1 \end{bmatrix}$$

$$\mathbf{X}_{m2} = \begin{bmatrix} 2 & -1 & 0 & 0 & -1 \\ 0 & -1 & 2 & -1 & 0 \\ -1 & -1 & 0 & -1 & 3 \end{bmatrix}, \mathbf{B} = \begin{bmatrix} -0.67 & 0.67 \\ 2.33 & -2.33 \\ -1.67 & 1.67 \end{bmatrix}, \mathbf{E} = \begin{bmatrix} 1 & -1 \\ 0 & 0 \\ 0 & 0 \end{bmatrix}$$

It can be seen, from matrix **E**, that by placing injection measurements at non-zero rows location, i.e., bus 1, the network becomes fully observable. This same methodology was implemented for measurement selection in IEEE 14-bus and IEEE 118-bus test systems, keeping the network observability intact.